Enhanced approach for simulation of rotor aerodynamic loads

K. Boorsma
F. Grasso
J.G. Holierhoek

Presented at: EWEA Offshore 2011, 29 November – 1 December 2011, Amsterdam, The Netherlands

ECN-M--12-003 FEBRUARY 2012

K. Boorsma · F. Grasso · J.G. Holierhoek

Enhanced approach for simulation of rotor aerodynamic loads

EWEA OFFSHORE 2011, December 2011

Abstract Uncertainty in aerodynamic load prediction is an important parameter driving the price of wind energy, especially for offshore locations. Blade Element Momentum (BEM) theory is the current standard for estimating the wind forces in load case calculations. The variety between the several engineering extensions used in different BEM implementations is huge. In addition to that, the assumption of radial independence of the annuli and the lack of wake modelling are well known shortcomings of this method. A more detailed approach to model the rotor aerodynamics is presented by a vortex line method with a free vortex wake. Contrary to the BEM method, it is possible to accurately simulate innovative rotor geometries exhibiting distributed control or non-straight blades.

A survey is made to investigate the influence of the various modelling options for several operating conditions. Firstly a rigid turbine is subject of investigation by means of a comparison to the NASA-AMES and MEXICO wind tunnel test databases. The predictive capability of the BEM modelling falls short for yawed flow and dynamic inflow cases. Coupling the aerodynamic solver to a structural dynamics code allows for a full aero-elastic wind turbine simulation in the time domain. The results are in agreement with measurements of a turbine at the ECN test site Wieringermeer. In addition to that the influence of the various modelling options on the aerodynamic damping is investigated. The research sheds new light on the uncertainties and capabilities of rotor aerodynamics modelling for design calculations. The long term benefit lies in improved guidelines for wind turbine design, thereby reducing the cost of offshore wind energy.

1 Introduction

Uncertainty in aerodynamic load prediction is an important parameter driving the price of wind energy, especially for offshore locations [1]. Blade Element Momentum (BEM) theory is the current standard for estimating the wind forces in load case calculations. The variety between the several engineering extensions used in different BEM implementations is huge [2,3]. In addition to that, the assumption of radial independence of the annuli and the lack of wake modelling are well known shortcomings of this method. A physically more correct approach to

K. Boorsma · F. Grasso · J.G. Holierhoek
Energy research Centre of the Netherlands, Westerduinweg 3, 1755 LE, Petten, Netherlands
Tel.: +31 (0) 224 564044
Fax: +31 (0) 224 568214
E-mail: boorsma@ecn.nl

model the rotor aerodynamics is presented by a vortex line method with a free vortex wake. Contrary to the BEM method, it is possible to accurately simulate innovative rotor geometries exhibiting distributed control or non-straight blades.

A survey is made to investigate the influence of the various modelling options for several operating conditions. Thereto the models used for this purpose are discussed in section 2. In section 3 a rigid turbine is subject of investigation by means of a comparison to the NASA-AMES and MEXICO wind tunnel test databases. This is followed by comparisons for a flexible turbine in section 4. The final conclusions are given in section 5.

2 Models

2.1 ECN AERO-MODULE

ECN has assembled the current state of the art of rotor aerodynamic models in the ECN AERO-MODULE. The two aerodynamic models included are the Blade Element Momentum (BEM) method similar to the implementation in PHATAS [4] and a free vortex wake code in the form of AWSM [5]. Several dynamic stall models, 3D correction models, wind modelling options and a module for calculating the tower effect are included. The package is to be coupled to arbitrary simulation software that solves the structural dynamics of a wind turbine. Blade position and velocity are given as an input to the ECN AERO-MODULE and forces and moments are then communicated back to the structural code. In addition to the coupled option, it is possible to run the software stand-alone for the purpose of aerodynamic calculations on a rigid turbine. An overview of the resulting program content is given in Figure 1.

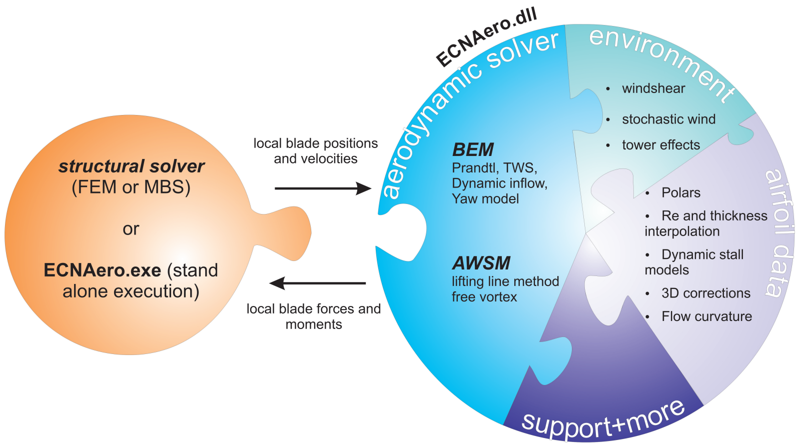

Fig. 1 Overview of the program content

2.1.1 BEM

Many different options exist for implementing a BEM formulation, especially with regard to the various engineering extensions. Within the ECN AERO-MODULE it is possible to switch off or vary many of these options, or use the default settings. The most important BEM extensions relevant to the current work are briefly highlighted below.

Oblique inflow To account for the variation of axial induction within each annulus, the model as defined by Schepers [6,7] and implemented in PHATAS [4] is employed. A skew function is determined for each element as a function of effective yaw angle, azimuth angle and radial location. This skew function then relates the local induction at each element to the annulus averaged axial induction. The skew function from the yaw model [6] was originally developed from the correlation between annulus averaged and local induction velocities for an annulus by means of wind tunnel measurements. The Glauert correction for yaw [8] currently is the basis for most available BEM codes. The main difference with the present model lies in the refinement between inboard and outboard sections through inclusion of the effects of the root vortex.

Prandtl correction To account for the finite number of blades, the Prandtl correction [9] (optionally for both root and tip) is calculated for each element. In its current implementation, axial wind speed, root- or tipvortex location and annulus averaged axial and tangential induction at the root or tip are necessary input for the evaluation of this function. The calculated Prandtl factor is incorporated in the iterative convergence procedure to relate the annulus averaged axial and tangential induction to the local induction at each element.

Dynamic inflow model The ECN dynamic inflow model [10] has been implemented. This model adds an extra term to the axial momentum equation to account for the aerodynamic rotor 'inertia' in the case of pitch action, rotational speed variation or wind speed variation.

2.1.2 AWSM

The Aerodynamic Windturbine Simulation Module (AWSM) has been developed at the Energy research Centre of the Netherlands (ECN) by van Garrel [5]. The main scope was to keep the advantages of BEM codes in terms of calculation time and ease of use, but to obtain a superior quality, especially concerning wake and time dependent wake-related phenomena. The AWSM code [5, 11, 12] is based on generalized lifting line theory in combination with a free vortex wake method. The main assumption in this theory is that the extension of the geometry in spanwise direction is predominant compared to the ones in chordwise and thickness direction. Because of this, the real geometry is represented by a line passing through the quarter chord point of each cross section. Hence the total flow field in chord-wise direction is concentrated in this point (Figure 2).

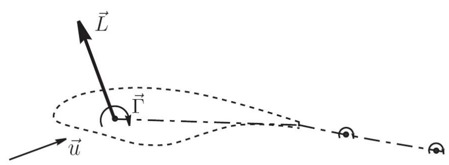

Fig. 2 Flowfield model

In AWSM, the effects of viscosity are taken into account through the user-supplied nonlinear relationship between local flow direction and local lift, drag and pitching moment coefficients. Along the lifting line, the generated elementary force can be determined by using the three-dimensional form of the Kutta-Jukowsky theorem. The two dimensional aerodynamic characteristics of the sections are known; this means that the elementary force can be calculated also from the sectional properties. By matching these two formulations, the lift along the blade can be obtained. The complete description can be found in [5].

Vortex wake As in the continuous flowfield representation, the vorticity is shed from the trailing edge of the configuration surface and convected downstream in the AWSM flow model as time advances. The blade geometry consists of one or more strips that carry a vortex ring whose bound vortices are located at the quarter chord position and at the trailing edge. The vortex strengths Γ of these vortex rings are to be determined. Each timestep Δt new vortex rings with these strengths are shed from the trailing edge and joined with the older vortex rings. These vortex rings together will form a vortex lattice. A sketch of the wake geometry for three strips after four timesteps is shown in Figure 3. The position of the first shed free spanwise vortex behind the trailing edge (TE) lies at some fraction between the current TE position and the wind-convected TE position from the previous timestep. Upstream of this position the vortex rings have a strength equal to the corresponding vortex ring at the configuration. The position of the downstream part of the wake is determined each timestep by convection of the wake vortex-lattice nodes.

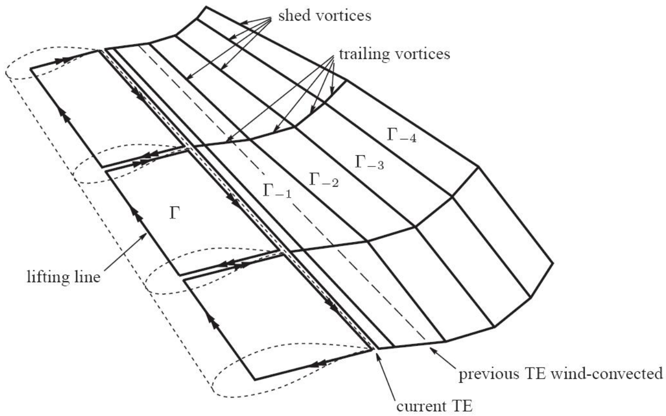

Fig. 3 Wake geometry

2.2 SIMPACK

SIMPACK [13] is a general purpose Multi-Body Simulation (MBS) software which can be used for the dynamic analysis of any mechanical or mechatronic system. Recently, SIMPACK also became popular amongst wind turbine manufacturers, for its calculation speed and extensive modelling freedom. The system can consist of both rigid bodies as well as flexible bodies with superimposed linear elastic deformation. It is up to the user to introduce flexibility by modal reduction and linearise around a specified state or to adopt a lumped mass or super-element approach including nonlinear effects.

3 Wind tunnel data

To be able to focus on the aerodynamic modelling, a comparison to available wind tunnel data has been performed. Both the NASA-AMES and MEXICO wind tunnel test database have been used, featuring turbine models which are considered to be rigid.

3.1 Computational settings

The BEM calculations feature a dynamic stall model [14], whereas AWSM does not. Apart from that, default settings are used for the BEM and AWSM simulations, which includes a 3D correction on the airfoil coefficients [15]. Furthermore it is worthwhile to mention that the time step of the AWSM simulations corresponds to a step of 10 $^\circ$ in rotor azimuth to reduce the computational effort. For the BEM simulations this figure amounts to about 2.5 $^\circ$.

3.2 Description of experiments

3.2.1 NASA-AMES

The National Renewable Energy Laboratory (NREL) tested a 10-meter diameter research wind turbine, denoted as NREL Phase VI wind turbine, in the NASA Ames 24.4 m $\times$ 36.6 m wind tunnel [16]. The wind turbine was extensively instrumented to characterize the aerodynamic and structural responses of a full-scale wind turbine rotor. Measured quantities included free stream conditions, airfoil aerodynamic pressure distributions, and machine responses. The turbine was tested in the tunnel in a 2-bladed, fixed-pitch (stall-controlled) configuration. Several configurations at different conditions have been measured but, in the present paper, only the data for 72 rpm, upwind rigid hub configuration are used. The blades have a nonlinear twist of 22.5 degrees and a linear taper with a maximum chord of 0.737 m at 25% span and 0.356 m at 100% span. This results in a relatively low aspect ratio and high solidity compared to modern (2 bladed) wind turbines. The NREL S809 airfoil was used along the total blade span.

3.2.2 MEXICO

Within the framework of the EU FP5 project MEXICO [1], a sophisticated aerodynamic experiment was designed, and executed in the Large Scale Low Speed Facility (LLF) of the German Dutch Wind tunnels (DNW). The experiment was designed for the 9.5 m $\times$ 9.5 m open test section of the LLF. A three bladed rotor model of 4.5 m diameter was designed and manufactured, including a speed controller and pitch actuator. The blades were twisted and tapered. The DU91-W2-250 airfoil was used at the root, the RISO-A1-21 airfoil at mid-span and the NACA64(3)418 airfoil at the outer part. The model was instrumented with 148 Kulite® pressure sensors, distributed over 5 sections of the blades; strain gauge bridges were applied to the three blade roots for the registration of bending moments in two directions. The model was mounted on the wind tunnel 6 components balance, where total forces and moments were measured. Finally a large number of PIV studies were performed to determine the flow field around the rotor, the inflow and near wake, and to track tip vortices.

3.3 Axial flow

Sectional forces are calculated for several axial flow operating conditions, varying tunnel speed and pitch angle. The most interesting results are illustrated in Figure 4, from design conditions to the turbulent wake state and separated flow conditions. The normal force F_n is orientated perpendicular to the chord, whilst the tangential force F_t is directed in line with the chord, positive pointing from leading edge to trailing edge.

Figure 4(a) and 4(b) show that for both the NASA-AMES and MEXICO test, the BEM and AWSM results are in good agreement with each other. For axial flow, the radial distribution of axial induction is designed to be constant along the blades, which validates the BEM assumption of radial interdependence between the annuli. The discrepancy between measurements and calculations is larger for the MEXICO than for the NASA-AMES experiment. This is not a new observation and topic of investigation in IEA Annex Mexnex(t) [17, 18].

Figure 4(c) shows the results of a special test case, where a standing vortex at inboard position was observed. The resulting spanwise discontinuity is more accurately taken into account by AWSM due to the inclusion of trailing vorticity between the elements. In addition to that, AWSM models the tip and root effects more accurately compared to the implemented Prandtl correction in BEM.

Figure 4(d) displays that correct input of sectional coefficients is difficult for separated flow conditions. Since these aerodynamic models greatly rely on this input, both methods fail in predicting the measured load distribution. The shortcoming of these aerodynamic models in separated flow conditions is in agreement with previous work [3].

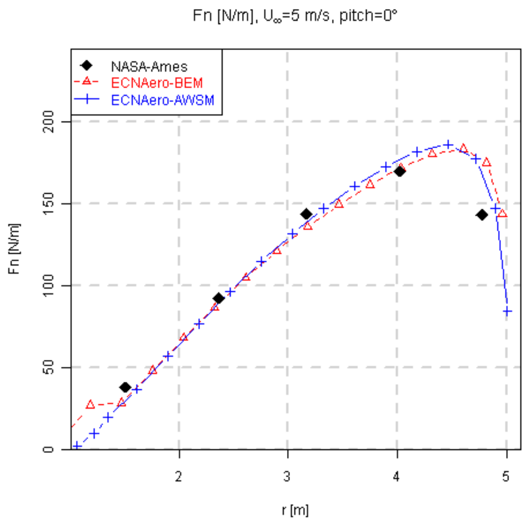

(a) NASA-AMES F_n, $U_\infty = 5$ m/s, pitch=0 °

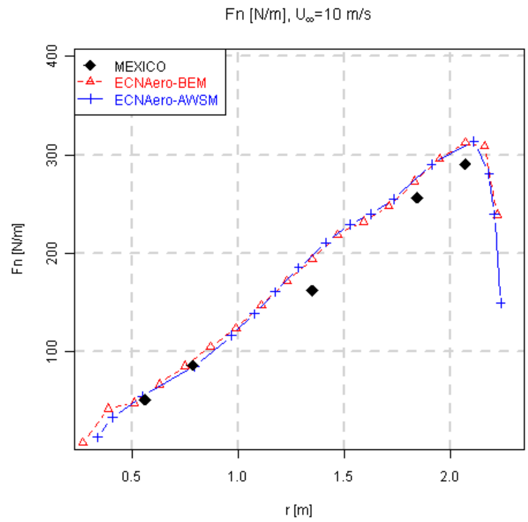

(b) MEXICO, F_n, $U_\infty = 15$ m/s, pitch=-2.3 °

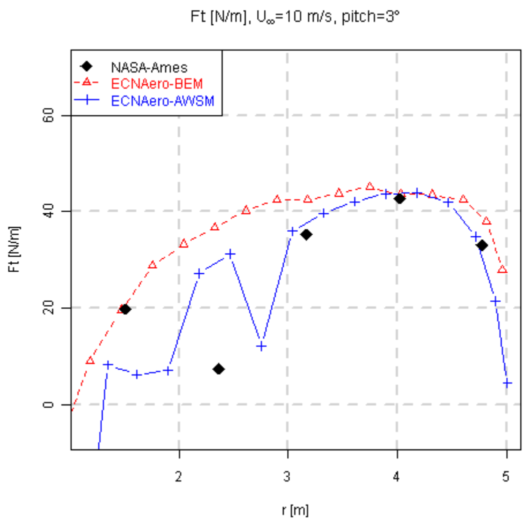

(c) NASA-AMES F_t, $U_\infty = 10$ m/s, pitch=3 °

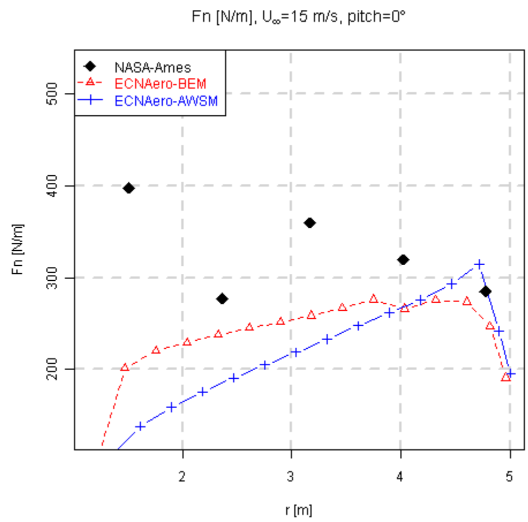

(d) NASA-AMES F_n, $U_\infty = 15$ m/s, pitch=0 °

Fig. 4 Radial distribution of sectional forces for axial flow conditions

3.4 Yawed flow

For yawed flow conditions sectional forces are displayed for a fixed radial position as a function of azimuth angle. Figure 5 shows a small selection from the available results. It is not surprising that the trend predicted by AWSM is in better agreement with the measurements than BEM. In a number of cases, the occurrence of dynamic stall effects for the inboard sections results in a worse trend prediction by AWSM. Addition of a dynamic stall model to the code is expected to resolve this issue.

The BEM results are in better agreement with the measurements than expected. It is believed that this can be attributed to the improved yaw modelling, which was previously confirmed

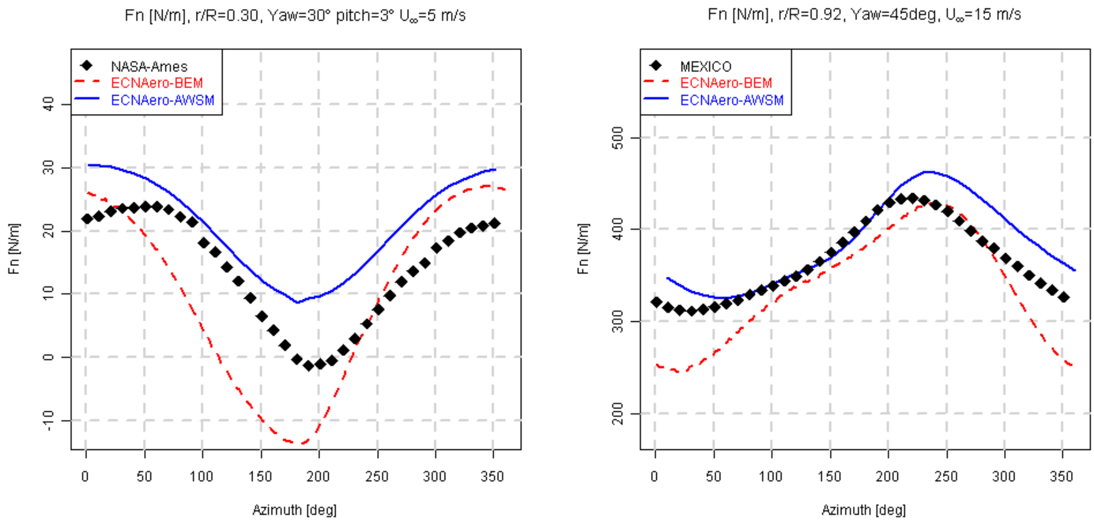

(a) NASA-AMES F_n, r/R=0.30, Yaw=30°, $U_\infty = 5$ m/s, pitch=3° (b) MEXICO F_n, r/R=0.92, Yaw=45°, $U_\infty = 15$ m/s, pitch=-2.3°

Fig. 5 Sectional force variation with rotor azimuth for yawed flow conditions

by comparing the current yaw model and the Glauert approach to experiments [6]. This provides extra confidence in the implemented yaw model for BEM as described in section 2.1.1

3.5 Dynamic inflow

In addition to the yawed flow cases, the NASA-AMES experiment included a pitch step test case to simulate a dynamic inflow situation. Figure 6 clearly shows the overshoot predicted by BEM and the correct representation of physics by AWSM in this case. Disabling the dynamic stall model for BEM to allow a more equal comparison has been confirmed not to influence the results for this case.

4 Flexible model

4.1 Model setup

A model has been created in SIMPACK that represents a real 2.5 MW wind turbine. The flexibility in the blades, tower and foundation are included in the model. A simple model of the drive train is also included and the wind turbine controls are represented in the model, the nacelle however is modelled as rigid. This model is coupled to the ECN AERO-MODULE and can run using the BEM modelling or AWSM modelling.

The real wind turbine on which the model is based, has been used in different measurement campaigns, where, amongst other, the moments near the blade roots are measured as well as the tower bottom moments, pitch setting and rpm. Meteorological masts that are situated in the field provide the necessary information concerning the wind speed and direction. From these sets of measurements, a set can be chosen where the wind turbine is operating at 0° yaw, at a relatively constant wind speed and not in the wake of another turbine. This situation can then be represented in the simulation allowing for a first validation of the model used.

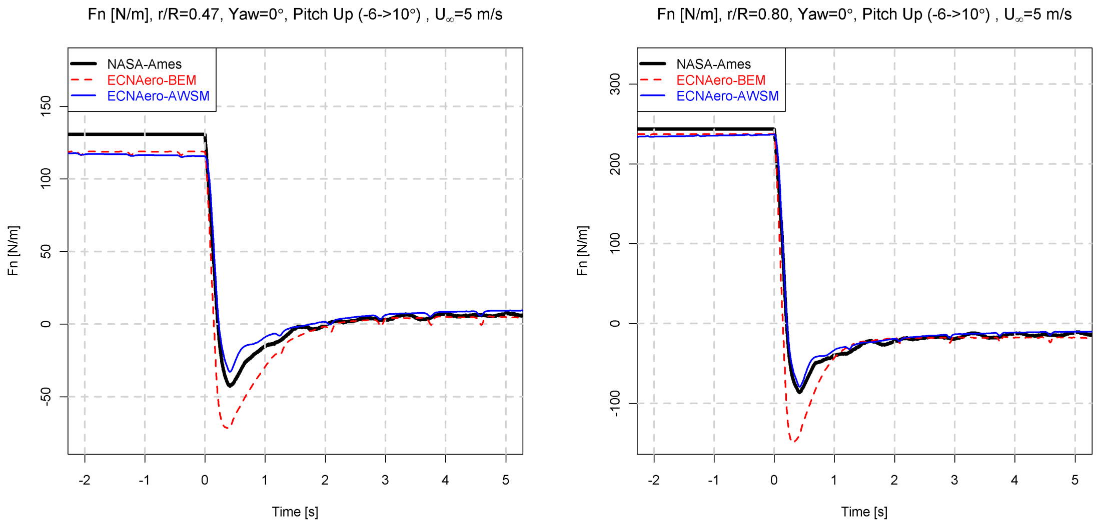

(a) F_n, r/R=0.47 (b) F_n, r/R=0.80

Fig. 6 NASA-AMES normal force variation with time for an upward pitching step, $U_\infty = 5$ m/s, pitch from -6 $^\circ$ to 10 $^\circ$

4.2 Validation using measurements

As discussed above, different sets of measured data were available for the validation of the SIMPACK plus ECN AERO-MODULE model. A set has been selected with a wind speed of around 15 m/s, a turbulence intensity of 16.21 % and a roughness length of 1.0386 m. Using SWIFT [19], a turbulent wind field was created to simulate the wind input. Of course this wind field does not represent the actual wind field in space and time, but when looking at power spectral densities, this will provide the possibility for validation.

The calculation using BEM, with the first order Snel dynamic stall model [14] was performed and the PSD's compared to the measured data. This is illustrated in Figure 7. In this figure the comparison between BEM and measured data is rather good. The frequencies that show up in the outcome are very similar. First the 1P frequency is clearly visible in all four results. The first edgewise blade frequency is also clearly visible in the results for the edgewise moments, it is around 6.5P. In the PSD of the flap moments, the 2P and 3P excitations are also visible and, though less pronounced than for the edgewise, the first flapwise frequency is visible around 3.5 - 4P. These results show that the combination of the SIMPACK model with the BEM model in the ECN AERO-MODULE is performing in accordance with the real turbine, when looking at the blade frequencies.

4.3 Pitch excitation

To investigate the difference between BEM and AWSM modelling when looking at a case where dynamic effects, such as dynamic inflow models, play an important role, simulations were performed for a wind turbine with a sudden change in pitch angle. This is similar to the case measured at NASA-AMES and discussed above, but what makes this case different is the flexibility of the structure and the fact that the blade will get to operate in stall. The sudden change in the pitch angle will have a large effect on the aerodynamic forces and therefore result in a change in the deformations of the wind turbine and these changes will again influence the

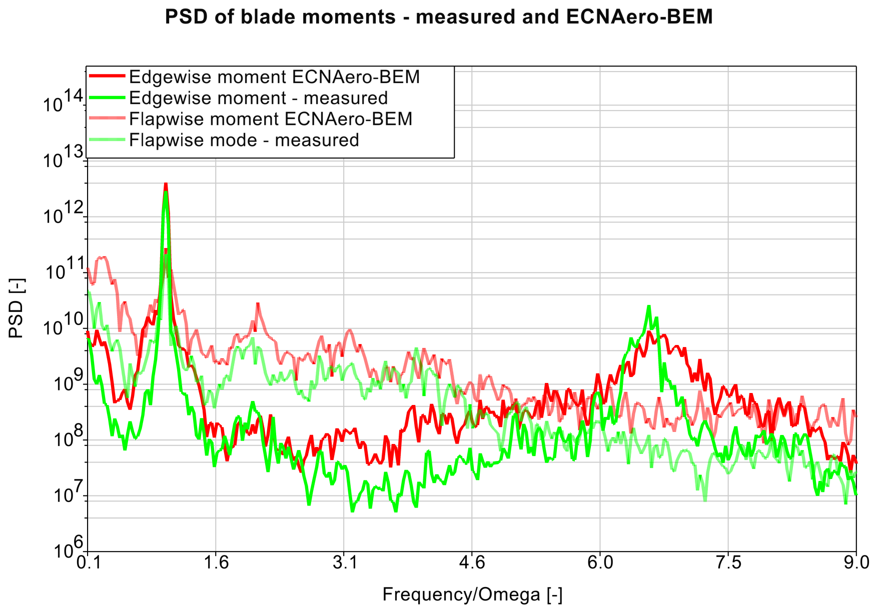

Fig. 7 A PSD of the measured and calculated edgewise and flapwise blade moments, for an undisturbed wind speed of 15 m/s.

aerodynamic forces. By comparing the results of the different models using steady wind, without turbulence, a comparison in the time domain becomes practical.

The aerodynamic power obtained in simulations with a pitch angle change from 0° to -15° at t=25 s is illustrated in Figure 8(a). This graph shows the results for BEM with the first order Snel dynamic stall model [14], BEM without dynamic stall and AWSM without dynamic stall model. The sudden pitch change results in large peaks in every simulation, however as shown in Figure 8(b) the peak is largest for the BEM modelling with dynamic stall included. The peak calculated using AWSM is the smallest of the three simulations.

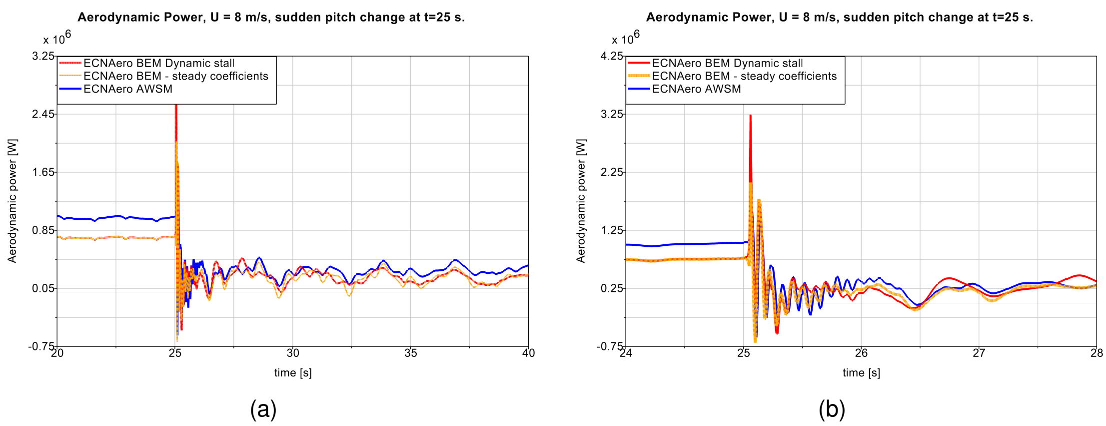

Fig. 8 Aerodynamic power of the turbine for U_∞=8 m/s and a pitch change after 25 seconds. The results using BEM (with and without dynamic stall model) and AWSM are shown, for two different time scales.

For an aeroelastic analysis, the damping is an important property. Therefore comparing the damping of the first fore/aft tower mode would be a good illustration of the difference between the aerodynamic models. The tower top position in fore/aft direction was used and by filtering out all other frequencies except a certain band width around the first fore/aft tower mode, it becomes possible to get an indication of the damping of this mode. The result is shown in Figure 9(a). It is expected that including a dynamic stall model will improve the damping of the flapwise modes as well as of this tower fore/aft mode. This is confirmed in the figure. However, using the more detailed AWSM model, which however does not include a dynamic stall model, shows the smallest damping.

The angles of attack along the radius of the blade at t=30 s are shown in Figure 9(b), the corresponding lift coefficients are also illustrated in this figure. This figure shows clearly that the angle of attack as determined in the simulation using AWSM is higher for the entire blade except for the tip. At these higher angles of attack, it is expected that the damping of the flapwise modes as well as the tower fore-aft mode will be smaller when compared to the BEM simulations. Especially as it is visible in the graph that the lift coefficient in smaller in the AWSM calculations, which means that the blade is operating beyond stall and c_{l_α} is actually negative.

The effect of the dynamic stall model on the lift coefficient is also visible, e.g. at 25 m radial position the two BEM simulations have an equal angle of attack, but there is a clear difference in the corresponding lift coefficient. The dynamic stall model increases the lift coefficient when the angle of attack is increasing in time. A sensible next step in the development would be

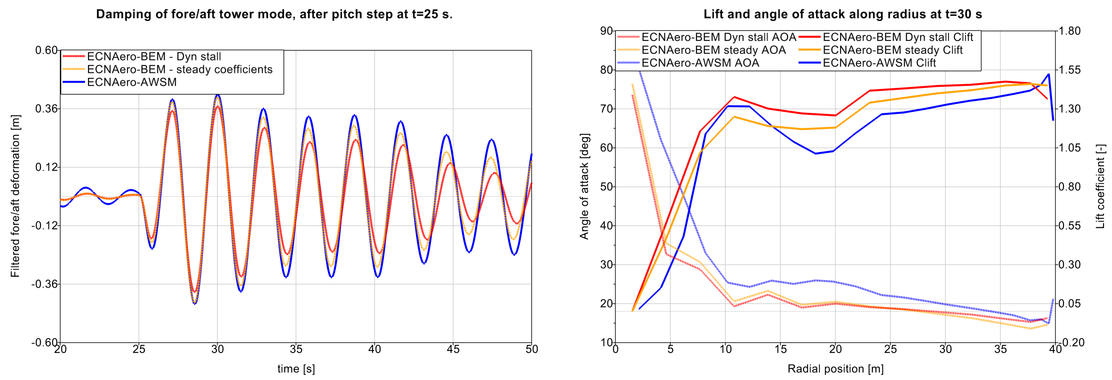

(a) (b)

Fig. 9 The filtered response of the tower top in fore/aft direction in time showing the damping of the excitation due to the pitch change (left) and the lift coefficient and angle of attack along the radius for t=30 s (right).

to implement a dynamic stall model in the AWSM model. However since the AWSM model already includes the influence of previously shed vortices, care should be taken not to model this effect in a dynamic stall model as well.

5 Conclusions

An extensive comparison of ECN AERO-MODULE BEM and AWSM to available wind tunnel measurements has been performed. The results point out the shortcomings of the models for several operating conditions. Most striking is the badly predicted overshoot and time constant by the BEM model in a sudden dynamic inflow change compared to the excellent agreement of AWSM for this case.

Simulations using the BEM and AWSM models, coupled to a flexible wind turbine model provided promising results. The comparison to the measured blade frequencies and the simulated frequencies for a test case was satisfactory and the dynamic effects of a sudden pitch change showed the expected difference between AWSM and BEM. Further investigations are needed to see if the AWSM model prediction is more accurate than the BEM model, as was the case for the NASA-AMES measurements with an upward pitch step change.

Acknowledgements

The work was partly funded by agentschap NL.

References

1. J.G. Schepers and H. Snel. Model experiments in controlled conditions, final report. Technical Report ECN-E–07-042, ECN, 2007.
2. J.G. Schepers et. al. “Verification of European Wind Turbine Design Codes”. ECN-C-01-055, ECN, April 2002.
3. D.A. Simms S. Schreck M.M. Hand L.J. Fingersh. “NREL Unsteady Aerodynamics Experiment in the NASA-Ames Wind Tunnel: A Comparison of Predictions to Measurements”. NREL/TP-500-29494, The National Renewable Energy Laboratory, NREL, June 2001.
4. C. Lindenburg and J.G. Schepers. Phatas-IV aeroelastic modelling, release ”dec-1999” and ”nov-2000”. Technical Report ECN-CX–00-027, ECN, 2000.
5. A. Van Garrel. Development of a wind turbine aerodynamics simulation module. Technical Report ECN-C–03-079, ECN, 2003.
6. J.G. Schepers and Vermeer L.J. Een engineering model voor scheefstand op basis van windtunnelmetingen. Technical Report ECN-CX–98-070, ECN, 1998.
7. J.G. Schepers. An engineering model for yawed conditions, developed on basis of wind tunnel measurements. Technical Report AIAA-1999-0039, AIAA, 1999.
8. H. Glauert. A general theory of the autogyro. *ARCR R&M*, nr 1111, 1926.
9. L. Prandtl and A. Betz. *Vier Abhandlungen zur hydrodynamik und aerodynamik*. Göttingen, Germany, 1927.
10. H. Snel and J.G. Schepers. Joule1: Joint investigation of dynamic inflow effects and implementation of an engineering model. Technical Report ECN-C–94-107, ECN, 1994.
11. F. Grasso. Awsm external field calculations. Technical Report ECN-X–09-043, ECN, 2009.
12. F. Grasso. Awsm ground and wind shear effects in aerodynamic calculations. Technical Report ECN-E–10-016, ECN, 2010.
13. http://www.simpack.com.
14. H. Snel. Heuristic modelling of dynamic stall characteristics. In *Conference proceedings European Wind Energy Conference*, pages 429–433, Dublin, Ireland, October 1997.
15. H. Snel, R. Houwink, J. Bosschers, W.J. Piers, G.J.W. Van Bussel, and A. Bruining. Sectional prediction of 3-d effects for stalled flow on rotating blades and comparison with measurements. In *Conference proceedings European Wind Energy Conference*, Lübeck-Travemünde, Germany, March 1993.
16. D. Simms, M. Hand, L.J. Fingersh, and D. Jager. Unsteady aerodynamics experiment phases II-IV test configurations and available data campaigns. Technical Report NREL/TP-500-25950, NREL, 1999.
17. J.G. Schepers, H. Snel and K. Boorsma. “IEA Task 29 Mexnext: Analysis of wind tunnel measurements from the EU project Mexico”. In *Proceedings of EAWE conference 'The Science of Making Torque from the Wind' held at Crete*, June 2010.
18. J.G. Schepers, Boorsma K, Bon A, Kim, C, Cho T. ”Results from Mexnext: Analysis of detailed aerodynamic measurements on a 4.5 m diameter rotor placed in the large German Dutch Wind Tunnel DNW”. In *Proceedings of European Wind Energy Conference, EWEC, held at Brussels*, March 2011.
19. D. Winkelaar. SWIFT: Program for three-dimensional wind simulation, part 1: Model description and program verification. Technical Report ECN-R–92-013, ECN, 1992.